

- A new primer, 5'-ACACGACGACCCGGCAGGTG-3', was derived from this sequence and used in combination with a λ ZAP-specific primer (Stratagene) to amplify a portion of the *ZMM2* (*ucsd78b*) transcript from our ear and tassel cDNA libraries (19). A full-length cDNA was subsequently isolated from the tassel library by screening at high stringency with a probe from the 3' end of the partial clone. RFLP analysis on recombinant inbreds confirmed that the correct locus had been obtained.
19. M. Mena, M. A. Mandel, D. R. Lerner, M. F. Yanofsky, R. J. Schmidt, *Plant J.* **8**, 845 (1995).
 20. G. Theissen, T. Strater, A. Fischer, H. Saedler, *Gene* **156**, 155 (1995).
 21. M. M. Goodman, C. W. Stuber, K. Newton, H. H. Weissinger, *Genetics* **96**, 697 (1980).
 22. J. F. Wendel, C. W. Stuber, M. D. Edwards, M. M. Goodman, *Theor. Appl. Genet.* **72**, 173 (1986).
 23. T. Helentjaris, D. Weber, S. Wright, *Genetics* **118**, 6442 (1989).
 24. J. L. Riechmann, B. A. Krizek, E. M. Meyerowitz, *Proc. Natl. Acad. Sci. U.S.A.* **93**, 4793 (1996).
 25. Abbreviations for the amino acid residues are as follows: A, Ala; C, Cys; D, Asp; E, Glu; F, Phe; G, Gly; H, His; I, Ile; K, Lys; L, Leu; M, Met; N, Asn; P, Pro; Q, Gln; R, Arg; S, Ser; T, Thr; V, Val; W, Trp; and Y, Tyr.
 26. T. A. Kiesselbach, *The Structure and Reproduction of Corn* [Univ. Nebr. Agric. Exp. Stn. Res. Bull. 161 (1949)].
 27. Analysis of RNA expression was performed as described in Fig. 1. A 500-base pair (bp) Hpa I-Nde I fragment was used as the ZAG1 probe in Fig. 4B. The *ZMM2*-specific probe (see below) was a 400-bp Xho I fragment isolated from the 3' end of the cDNA. Both probes were labeled to comparable specific activities. The faint *ZMM2* hybridization detected in endosperm is likely a result of nucellar tissue, which often contaminates endosperm tissue obtained from early developmental stages. RNA from immature ears and tassels was isolated from developing inflorescences that were <3 cm in length. Hybridization with a tubulin probe produced signal in every lane.
 28. We thank T. Fox and M. Albertson for use of their tassel cDNA library. Supported in part by postdoctoral fellowships from the North Atlantic Treaty Organization and Ministerio de Educación y Ciencia (to M.M.) and from the Pioneer Discovery Research Program (to R.B.M.) and by grants from the U.S. Department of Agriculture and the University of California Biotechnology and Research Foundation (to R.J.S. and M.F.Y.).

5 July 1996; accepted 13 September 1996

CRNF, a Molluscan Neurotrophic Factor That Interacts with the p75 Neurotrophin Receptor

M. Fainzilber,* A. B. Smit, N. I. Syed, W. C. Wildering, P. M. Hermann, R. C. van der Schors, C. Jiménez, K. W. Li, J. van Minnen, A. G. M. Bulloch, C. F. Ibáñez, W. P. M. Geraerts

A 13.1-kilodalton protein, cysteine-rich neurotrophic factor (CRNF), was purified from the mollusk *Lymnaea stagnalis* by use of a binding assay on the p75 neurotrophin receptor. CRNF bound to p75 with nanomolar affinity but was not similar in sequence to neurotrophins or any other known gene product. CRNF messenger RNA expression was highest in adult foot subepithelial cells; in the central nervous system, expression was regulated by lesion. The factor evoked neurite outgrowth and modulated calcium currents in pedal motor neurons. Thus, CRNF may be involved in target-derived trophic support for motor neurons and could represent the prototype of another family of p75 ligands.

The survival, differentiation, and plasticity of vertebrate neurons are influenced by neurotrophic factors, the best characterized

M. Fainzilber, Laboratory of Molecular Neurobiology, Department of Neuroscience, Karolinska Institute, Berzelius Laboratories Building, Doktorsringen 12A, S-17177 Stockholm, Sweden, and Graduate School Neurosciences Amsterdam, Institute of Neuroscience, Vrije Universiteit, de Boelelaan 1087, 1081 HV Amsterdam, Netherlands.

A. B. Smit, R. C. van der Schors, C. Jiménez, K. W. Li, J. van Minnen, W. P. M. Geraerts, Graduate School Neurosciences Amsterdam, Institute of Neuroscience, Vrije Universiteit, de Boelelaan 1087, 1081 HV Amsterdam, Netherlands.

N. I. Syed, W. C. Wildering, P. M. Hermann, A. G. M. Bulloch, Neuroscience Research Group, University of Calgary, 3330 Hospital Drive, Calgary, Alberta T2N 4N1, Canada.

C. F. Ibáñez, Laboratory of Molecular Neurobiology, Department of Neuroscience, Karolinska Institute, Berzelius Laboratories Building, Doktorsringen 12A, S-17177 Stockholm, Sweden.

*To whom correspondence should be addressed at the Karolinska Institute. E-mail: michael@cajal.mbb.ki.se

of which are the neurotrophins (1). Invertebrate neuronal systems have provided useful models for development and regeneration of the nervous system; however, efforts to clone neurotrophin or neurotrophin receptor-like sequences in invertebrates have so far been unsuccessful (2). Indeed, it has been argued that neurotrophic factors may be a comparatively late addition to the arsenal of mechanisms controlling nervous system development and regeneration, and that such factors may be required only in long-lived organisms with complex nervous systems (2). To examine the existence of neurotrophin-related molecules in an invertebrate, we focused on the snail *Lymnaea stagnalis*, which is used as a model in cellular and molecular neuroscience (3, 4). *Lymnaea* hemolymph or central nervous system (CNS)-conditioned medium (CM) evoke neurite outgrowth from snail motor neu-

rons. This activity can be mimicked by murine nerve growth factor (NGF), which furthermore has acute effects on calcium currents in *Lymnaea* neurons (4).

Initial attempts to clone a *Lymnaea* neurotrophin homolog by polymerase chain reaction (PCR) on the basis of conserved regions of vertebrate neurotrophins (5) were not successful. Therefore, we adopted a functional approach to target neurotrophin family members. All neurotrophins interact with two receptor types—ligand-specific receptor tyrosine kinases of the Trk family (6) and a shared receptor termed p75 (7). Starting from the premise that a putative molluscan neurotrophin homolog might also bind to the p75 receptor, we assayed *Lymnaea* CM and hemolymph for inhibition of binding of ¹²⁵I-labeled NGF to A875 human melanoma cells, which express high levels of p75 but no Trk receptors. Hemolymph and CM-derived fractions inhibited NGF binding to p75 in a dose-dependent manner (Fig. 1A). Further fractionation revealed that NGF-displacing fractions from both CM and hemolymph had identical chromatographic elution properties and contained an almost identical protein mass of 13.1 kD.

The higher amounts of the 13.1-kD protein in hemolymph enabled its purification to homogeneity from a pool of 7 liters of snail hemolymph, using matrix-assisted laser desorption ionization mass spectrometry (MALDI-MS) to monitor the purification (8). The final purified fraction (Fig. 1B) contained a major component of 13.1 kD and a minor component of 13.97 kD, as analyzed by MALDI-MS (Fig. 1C). Internal and NH₂-terminal peptide sequences of both proteins were identical and novel. These sequences served to design primers for PCR and eventual isolation of a cDNA clone (9), which encoded an open reading frame of 121 amino acids, including an 18-residue putative signal sequence followed by a mature product of 103 amino acids containing all the peptide sequences previously obtained (Fig. 1E). The sequence was not significantly similar to any known protein or DNA sequence in the public databases. The protein molecular mass predicted from the cDNA sequence is 12.5 kD, which is close to the measured masses of the purified CRNF isoforms and suggests that the latter may arise from different extents of glycosylation on the single consensus N-glycosylation site (Fig. 1E). The sequence contained a high number of cysteine residues, comprising over 10% of the protein, hence the name CRNF (cysteine-rich neurotrophic factor).

An anti-peptide antiserum was raised (9) against a synthetic peptide based on the COOH-terminal region of the CRNF se-

quence. Immunoreactive bands with apparent electrophoretic mobilities of 14 to 16 kD were observed upon protein immunoblotting of *Lymnaea* foot tissue homogenates (Fig. 1D). This antiserum was subsequently used to monitor production of recombinant CRNF in baculovirus-infected insect cells (9). Recombinant CRNF was readily produced in baculovirus-infected insect cells, but was not secreted, and could be identified in cell lysates as two major immunoreactive bands with apparent molecular masses of 18 and 24 kD (Fig. 1D). No CRNF immunoreactivity could be found in mock-infected cells. The larger apparent mass of the protein produced in baculovirus could be due to incomplete processing of the signal peptide in the insect cells or to a higher extent of glycosylation.

Both native and recombinant CRNF inhibited binding of ¹²⁵I-NGF to p75 in a dose-dependent manner with measured median inhibitory concentrations (IC₅₀'s) of approximately 15 nM for the native protein and 45 nM for recombinant CRNF (Fig. 2A). CRNF displacement of NGF from p75 could be mediated by a number of different mechanisms, including competitive binding of CRNF to p75 or a direct interaction between CRNF and NGF. We used surface plasmon resonance (10) to determine directly whether CRNF can interact with

NGF or with a soluble p75 extracellular domain (Sp75) (11). NGF or CRNF were immobilized separately on BIAcore sensor chips, and these chips were subsequently used to monitor binding of the other ligand or of Sp75. No interaction between NGF and CRNF was observed. In contrast, Sp75 bound comparably to both immobilized NGF or CRNF, whereas no binding was observed on control chips (Fig. 2B). Titration of Sp75 binding to CRNF (Fig. 2C) enabled calculation of *k*_{off} and *k*_{on} from the dissociation and association phases of the curves, respectively. The apparent equilibrium dissociation constant (*K*_d) subsequently calculated from these kinetic measurements was 50.9 ± 9.7 nM, which is in the same range as the IC₅₀ for competitive displacement of NGF from A875 cells.

In order to gain insight into possible physiological roles of CRNF, we examined its mRNA expression in various tissues of the adult snail by ribonuclease protection assays (RPAs). High CRNF mRNA expression was almost exclusively restricted to the foot, with low levels in mantle tissue (Fig. 3A). In addition, CRNF expression could be induced by mechanical lesion of CNS explants in vitro (Fig. 3B), suggesting a role for CRNF in injury repair. In situ hybridization was performed to localize CRNF expression sites in the peripheral tissues

comprising the foot. Intense labeling was observed in a distinct layer of large globular subepithelial cells (Fig. 3C). This region of the foot has extensive arborization from the pedal nerves on the way to their target cells (12).

The highly restricted pattern of expression of CRNF mRNA in adult foot might indicate trophic roles for this molecule on peripheral and pedal neurons innervating the foot. Adult *Lymnaea* neurons are not dependent on exogenous trophic factors for survival in vitro, and furthermore, developmental programmed cell death has not been observed in molluscan CNS (13). However, trophic activity in molluscan neurons can readily be monitored as neurite outgrowth in isolated neuronal cultures (3, 4). CRNF activities were examined, using *Lymnaea*

Fig. 1. Identification and purification of CRNF.

(A) *Lymnaea* hemolymph (HL, gray bars) and CM-derived fractions (black bars) inhibit binding of ¹²⁵I-NGF to p75 receptors on A875 melanoma cells in a dose-dependent manner. Striped bar indicates control. (B) Final reverse-phase high-performance liquid chromatography step in the purification of CRNF, Vydac C4, with a flow of 1 ml/min. Gradient of acetonitrile in aqueous 0.1% TFA is shown by dashed line; CRNF fraction is indicated by shading under the peak. (C) MALDI-MS on the purified peak reveals two protein masses of 13.10 and 13.97 kD. (D) SDS-polyacrylamide gel electrophoresis of purified CRNF under reducing conditions reveals two bands upon Coomassie staining after blotting (lane 1). An antiserum to CRNF peptide identified a 14- to 16-kD band on protein immunoblots of extracts of *Lymnaea* foot tissues (lane 2). Insect cells infected with a CRNF-recombinant baculovirus revealed immunoreactive bands of higher apparent mass in insect cell lysates (lane 4), but not in conditioned medium (lane 3). Molecular size markers are indicated. (E) Amino acid sequence of CRNF, as predicted from the cDNA clone. The putative signal sequence is in italics, cysteine residues are in bold, one consensus site for N-linked glycosylation is indicated by an asterisk, and the stop codon is indicated by a dot. Sequences corresponding to the peptides previously obtained by Edman degradation are underlined. Single-letter amino acid abbreviations are as in (18).

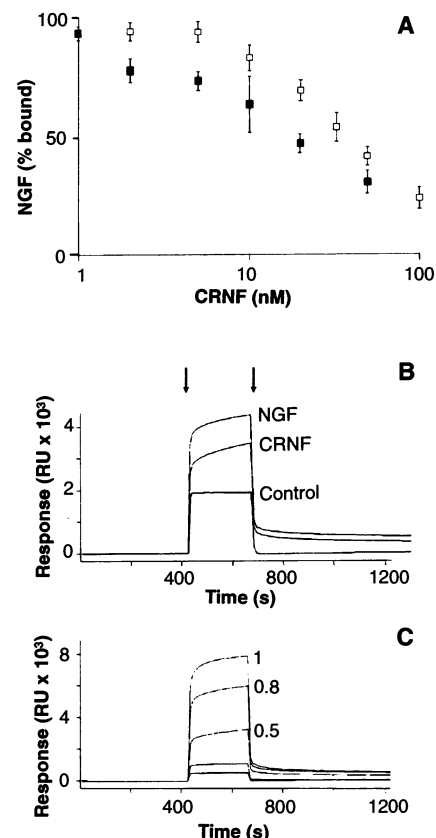
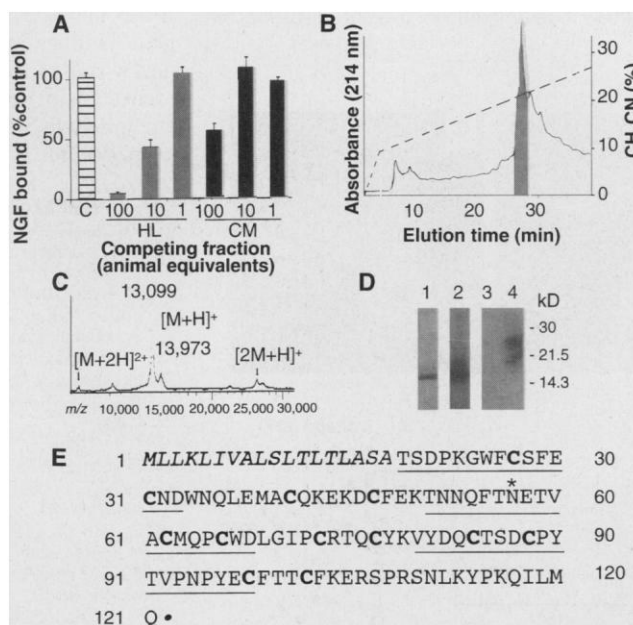


Fig. 2. Binding of CRNF to the p75 neurotrophin receptor. (A) Inhibition of ¹²⁵I-NGF binding to A875 cells (19) by native (solid squares) and recombinant CRNF (empty squares). (B) Surface plasmon resonance measurement of the interaction of 0.5 μM soluble p75 extracellular domain (Sp75) with control chips, and chips on which NGF or CRNF was immobilized (20). Arrows indicate start and ending of Sp75 application. Note the association and dissociation curves observed on NGF or CRNF chips, in contrast to the unspecific mass effect seen on the control chip. RU, resonance units. (C) Titration of Sp75 interaction with immobilized CRNF. Concentrations of Sp75 in μM are indicated for each trace.

pedal A motor neurons (PedA), which are a potential target population for this factor. Purified CRNF evoked neurite outgrowth from PedA neurons in vitro (Fig. 4, A through C), with responses including neurons that displayed multiple short neurites tipped with small growth cones (Fig. 4B), whereas other neurons formed large growth cones that approached the cell body in diameter (Fig. 4C). This response peaked within 24 hours and was dose dependent, with a maximal effective concentration of

25 pM (Fig. 4D). The lower response seen at higher doses of CRNF is reminiscent of the bell-shaped dose-response relationships previously reported for several vertebrate trophic factors in outgrowth assays [for example, (14)].

Murine NGF enhances high-voltage activated (HVA) calcium currents in *Lymnaea* Parietal A motor neurons (ParA), within seconds of application (4). Therefore, we examined the effects of CRNF on HVA calcium currents in ParA neurons.

Superfusion of ParA neurons in vitro with 1 nM CRNF modulated the HVA calcium currents in 50% of the cells tested ($n = 8$). In ParA cells expressing both fast- and slow-inactivating calcium currents, CRNF enhanced the peak calcium current (Fig. 4E). The current-to-voltage relation (Fig. 4F) illustrates that the effect of CRNF was primarily on the fast-inactivating current, whereas the slow-inactivating current remained largely unaffected. In contrast to previous observations with murine NGF, the effects of CRNF on the HVA calcium currents did not reverse within a few minutes of washing. Thus, CRNF differentially modulated the various components of HVA calcium currents expressed in *Lymnaea* motor neurons, and may play a role in plasticity-related processes in *Lymnaea* CNS.

We propose that CRNF is an invertebrate neurotrophic factor (15) because it is expressed in a restricted pattern and, at low levels, it has trophic and plasticity-related activities at low concentrations on potential target neurons and was identified on the basis of its interaction with the p75 neurotrophin receptor. CRNF shares no obvious sequence similarity with mammalian neurotrophins, suggesting that properties in common between these two families may have arisen from convergent evolution. Alternatively, as our data do not rule out the possibility that neurotrophins exist in *Lymnaea*, CRNF may represent the prototype of a novel family of p75 ligands. A number of gene families important in axon guidance and wiring of the nervous system were first identified in invertebrates (16); therefore, the phyletic distribution of CRNF is of primary interest.

Fig. 3. Expression of CRNF mRNA in adult *Lymnaea* tissues. (A) RPA on 5 μ g total RNA from different adult tissues revealed high expression of CRNF mRNA in the foot and lower levels in mantle tissue (overnight exposure) (21). Position of a 380-nucleotide band is indicated. (B) RPA analysis of CRNF mRNA in control CNS compared to CNS after 36 hours in culture and cultured CNS after crush lesion to the interganglionic connectives and commissures. We used 20 μ g total RNA from each sample, and exposure time was 7 days. (C) Localization of CRNF mRNA expression in adult foot by in situ hybridization. Intense signal was observed in a layer of large subepithelial cells. No signal was detected using a control probe. (E, epithelial layer; Ct, connective tissue layer; scale bar, 50 μ m.)

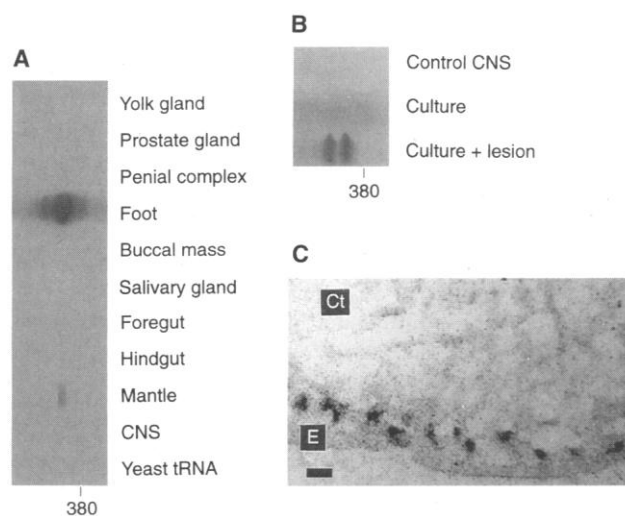
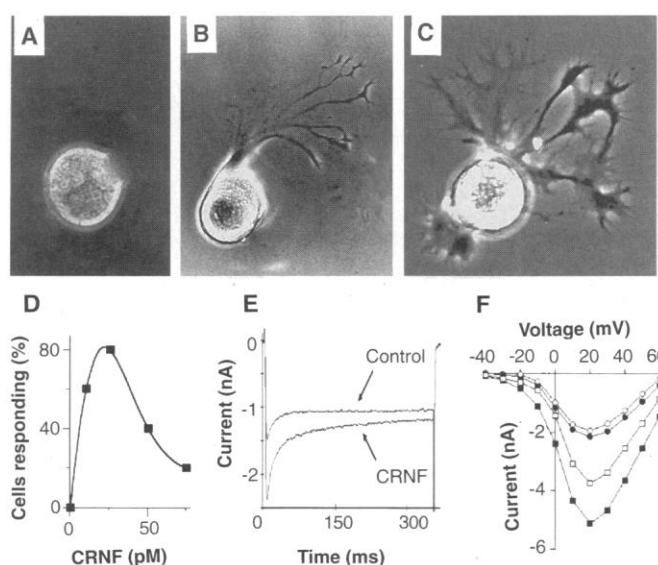


Fig. 4. Effects of CRNF on *Lymnaea* motor neurons. (A through D) CRNF evokes neurite outgrowth from cultured PedA motor neurons. (A) Control cultures showed no neurite extension. (B and C) Neurons developed processes and growth cones 24 hours after treatment with CRNF. (D) Dose-response relation of the number of cells exhibiting neurite outgrowth in response to CRNF ($n = 6$ for each data point). (E and F) Modulation of HVA calcium currents in Right Parietal A motor neurons by CRNF. (E) Calcium current recorded under whole-cell clamp techniques at a test potential of 0 mV (holding potential of -80 mV) before application of CRNF (control) and 10 min after the start of an application of 1 nM CRNF. The early peak current was markedly increased in the presence of CRNF. (F) Current-to-voltage relations of peak (squares) and late (circles) currents show that the effect of CRNF appears restricted to the peak current. Open symbols are peak and late current values prior to CRNF application and filled symbols are values 10 min after the start of CRNF application. Methods were as described (4).



REFERENCES AND NOTES

- C. F. Ibáñez et al., Eds., *Life and Death in the Nervous System* (Elsevier, Oxford, 1995); H. Thoenen, *Science* **270**, 593 (1995); S. Cohen-Corey and S. E. Fraser, *Nature* **378**, 192 (1995); H. Kang and E. M. Schuman, *Science* **273**, 1402 (1996).
- Y.-A. Barde, *J. Neurobiol.* **25**, 1329 (1994).
- N. I. Syed, A. G. M. Bulloch, K. Lukowiak, *Science* **250**, 282 (1990); N. I. Syed et al., *Neuron* **8**, 767 (1992).
- R. L. Ridgeway, N. I. Syed, K. Lukowiak, A. G. M. Bulloch, *J. Neurobiol.* **22**, 377 (1991); W. C. Wildering, J. C. Lodder, K. S. Kits, A. G. M. Bulloch, *J. Neurophysiol.* **74**, 2778 (1995).
- F. Halböök, C. F. Ibáñez, H. Persson, *Neuron* **6**, 845 (1991); R. Götz, F. Raulf, M. Scharlt, *J. Neurochem.* **59**, 432 (1992).
- M. Barbacid, *J. Neurobiol.* **25**, 1386 (1994).
- M. V. Chao, *ibid.*, p. 1373; M. Bothwell, *Science* **272**, 506 (1996).
- Hemolymph was milked from adult *Lymnaea* by collecting fluid ejected after tapping the foot. The final 7-liter pool of hemolymph represented approximately 16,000 animal milkings. Aliquots of 1 liter were processed as follows: (i) Ultracentrifugation for 2 hours at 120,000g to precipitate hemocyanin. (ii) Supernatant was applied to Polybuffer 94 (Pharmacia) equilibrated and washed with 20 mM tris (pH 7.9). Bound proteins were eluted by 1 M NaCl, and desalted and concentrated with Poros 20 R1. (iii) Eluted

- fractions were applied to linked Beckman SW2000-SW3000 molecular exclusion columns, equilibrated, and eluted with 0.5× phosphate-buffered saline/15% acetonitrile. (iv) Fractions eluting at apparent masses of 20 to 30 kD were loaded onto fast-flow reverse-phase Poros 20 R1 equilibrated at 4 ml/min in 15% acetonitrile/0.1% trifluoroacetic acid (TFA). After a 2-min wash, the bound proteins were eluted with a linear gradient from 15 to 60% acetonitrile in 2 to 24 min. (v) Fractions eluting from Poros R1 at 32 to 36% acetonitrile were refractionated on wide-pore Vydac C4 (250 mm by 4.6 mm, 5 μm particle size) at 1 ml/min, in a gradient of acetonitrile in 0.1% TFA (Fig. 1B). Amino acid sequence analysis was performed on blotted Coomassie stained bands, or reverse phase purified peptides from Endo-LysC digest, by automated Edman degradation on an Applied Biosystems 473A system. Methods for MALDI-MS were as described (17).
9. Degenerate oligonucleotide primers encoding all possible codons for TSDPKGWF (18) (sense, NH₂-terminal) and PYTVPNPY (18) (antisense, internal peptide sequence) were used for PCR on *Lymnaea* CNS cDNA. A 230-base pair (bp) product was cloned, sequenced, and used to screen a CNS cDNA library, resulting in isolation of a 472-bp cDNA clone. The nucleotide sequence of CRNF has been deposited in Genbank (accession number U72990). Mouse polyclonal antisera were raised against RSNLKYPKQLLM (18) (residues 109 through 120 of the amino acid sequence). An expression construct was made by PCR amplification of the CRNF coding region, which was subcloned into pBAC (Clontech). Recombinant baculovirus were generated from the pBAC construct, using Clontech reagents according to manufacturer's instructions. Recombinant protein was produced in baculovirus-infected insect cells (19) and purified according to (8).
 10. R. J. Fisher and M. Fivash, *Curr. Opin. Biotechnol.* **5**, 389 (1994).
 11. G. Weskamp and L. F. Reichardt, *Neuron* **6**, 649 (1991).
 12. N. I. Syed and W. Winlow, *Comp. Biochem. Physiol. A Comp. Physiol.* **93**, 633 (1989); A. R. Jackson, T. H. Macrae, R. P. Croll, *Cell Tissue Res.* **281**, 507 (1995).
 13. R. Marois and T. J. Carew, *J. Neurobiol.* **21**, 1053 (1990).
 14. M. Trupp *et al.*, *J. Cell. Biol.* **130**, 137 (1995).
 15. S. Korsching, *J. Neurosci.* **13**, 2739 (1993).
 16. C. S. Goodman, *Cell* **78**, 353 (1994); *Annu. Rev. Neurosci.* **19**, 341 (1996).
 17. C. R. Jiménez *et al.*, *J. Neurochem.* **62**, 404 (1994).
 18. Single-letter abbreviations for the amino acid residues are as follows: A, Ala; C, Cys; D, Asp; E, Glu; F, Phe; G, Gly; H, His; I, Ile; K, Lys; L, Leu; M, Met; N, Asn; P, Pro; Q, Gln; R, Arg; S, Ser; T, Thr; V, Val; W, Trp; and Y, Tyr.
 19. M. Rydén *et al.*, *EMBO J.* **14**, 1979 (1995).
 20. Immobilization of NGF or CRNF to BIAcore CM5 sensor chips was done by amine coupling in 20 mM acetate buffer (pH 5.6 or 3.6). Binding of Sp75 to immobilized ligand was monitored in a BIAcore 2000 Biosensor (Pharmacia) at 20°C, with a flow of 5 ml/min, in Hepes-buffered saline. Kinetic analyses were done with BIAevaluation software, version 2.0 (Pharmacia).
 21. Riboprobes for RPA and in situ hybridization were generated from linearized 380-bp subclones of CRNF cDNA in pCDNA3 (Stratagene). RPA was per-

formed with equal amounts of total RNA, using RPAII reagents (Ambion). Equal loading was verified on ethidium bromide-stained gels and by parallel RPA with riboprobes for ubiquitously expressed *Lymnaea* mRNAs [fructose 1,6-biphosphate aldolase (Genbank accession number U73114) for the experiment of Fig. 3A and a CNS tyrosine kinase (A. G. M. Bulloch, unpublished data) for Fig. 3B].

22. Dedicated to the memory of Professor Håkan Persson (1952–1993), who was one of the most enthusiastic initiators of this project. We thank G. Hauser, R. van Elk, A.-S. Nilsson, E. van Kesteren, C. Popelier, and A. Ahlsen for technical support; L. Johanson and T. Laan for secretarial help; A. Vlamis and A. Holmgren for their generous assistance with the BIAcore; K. Dreisewerd and F. Hillenkamp for sharing expertise in MALDI-MS; and all members of the Molecular Neurobiology group at Vrije Universiteit Amsterdam for cheerful assistance in snail milking. Sp75 baculovirus and antisera were the generous gift of G. Weskamp and L. Reichardt. Supported by grants from the Swedish Medical Research Council (MRC), the European Neuroscience Program, the Canadian MRC, the Canadian Neuroscience Network, the Canadian National Science and Engineering Research Council, and a special equipment grant from the Netherlands Organization for Research. M.F. was supported by a long-term fellowship from the European Molecular Biology Organization and subsequently by the Swedish MRC. A.G.M.B., N.I.S., and W.C.W. were supported by the Alberta Heritage Foundation for Medical Research.

6 August 1996; accepted 4 October 1996

T Cell Telomere Length in HIV-1 Infection: No Evidence for Increased CD4⁺ T Cell Turnover

Katja C. Wolthers, G. Bea A. Wisman, Sigrid A. Otto, Ana-Maria de Roda Husman, Niels Schaft, Frank de Wolf, Jaap Goudsmit, Roel A. Coutinho, Ate G. J. van der Zee, Linde Meyaard, Frank Miedema*

Progression to acquired immunodeficiency syndrome (AIDS) has been related to exhaustion of the regenerative capacity of the immune system resulting from high T cell turnover. Analysis of telomeric terminal restriction fragment (TRF) length, a marker for cellular replicative history, showed that CD8⁺ T cell TRF length decreased but CD4⁺ T cell TRF length was stable during the course of human immunodeficiency virus type-1 (HIV-1) infection, which was not explained by differential telomerase activity. This observation provides evidence that turnover in the course of HIV-1 infection can be increased considerably in CD8⁺ T cells, but not in CD4⁺ T cells. These results are compatible with CD4⁺ T cell decline in HIV-1 infection caused by interference with cell renewal.

In the course of HIV-1 infection, CD4⁺ T cells are progressively lost, CD8⁺ T cell numbers gradually increase, and immune function is progressively disturbed (1). Chronic immune activation is reflected by an activated phenotype of CD8⁺ T cells in blood and lymph nodes (2), high concentrations of circulating HIV-specific cytotoxic T lymphocyte (CTL) effectors that are highly activated (3), and activation-induced programmed cell death that affects both CD8⁺ and CD4⁺ T cells (4). CD4⁺ T cell numbers decline at an accelerated rate about 1.5 to 2 years be-

fore the onset of AIDS (5). It has been proposed that HIV-induced rapid CD4⁺ T cell turnover eventually leads to exhaustion of the regenerative capacity of the immune system (6, 7).

To study T cell turnover, we analyzed telomeric TRF length. Telomeres are the extreme ends of chromosomes that consist of TTAGGG repeats, ~10 kb long in humans (8). After each round of cell division telomeric sequence is lost (9–12) because of the inability of DNA polymerases to fully replicate the 5' end of the chromosome

(13). Cross-sectional studies have revealed a loss of 30 to 50 base pairs (bp) per year for human leucocytes in vivo (9, 10, 14), and telomere length has been used as a marker for replicative history and the proliferative potential of cells (9–11, 15, 16). To overcome the considerable variation in lymphocyte telomere length between donors of the same age (17), we analyzed TRF length on sequential peripheral blood mononuclear cell (PBMC) samples. For these analyses, the subtelomeric probe pTH2Δ (18) was chosen because it does not result in disproportionately high signals for longer telomeric

K. C. Wolthers, S. A. Otto, A.-M. de Roda Husman, N. Schaft, L. Meyaard, Department of Clinical Viro-Immunology, Central Laboratory of the Netherlands Red Cross Blood Transfusion Service and Laboratory for Experimental and Clinical Immunology of the University of Amsterdam, Amsterdam, Netherlands.

G. B. A. Wisman and A. G. J. van der Zee, Department of Gynaecology and Obstetrics, Academic Hospital Groningen, University of Groningen, Groningen, Netherlands.

F. de Wolf and J. Goudsmit, Department of Human Retrovirology, Academic Medical Centre, University of Amsterdam, Amsterdam, Netherlands.

R. A. Coutinho, Department of Public Health, Municipal Health Service, Amsterdam, Netherlands.

F. Miedema, Department of Clinical Viro-Immunology, Central Laboratory of the Netherlands Red Cross Blood Transfusion Service and Laboratory for Experimental and Clinical Immunology of the University of Amsterdam, Amsterdam, Netherlands, and Department of Human Retrovirology, Academic Medical Centre, University of Amsterdam, Amsterdam, Netherlands.

*To whom correspondence should be addressed at Central Laboratory of the Netherlands Red Cross Blood Transfusion Service, Department of Clinical Viro-Immunology, Plesmanlaan 125, 1066 CX Amsterdam, Netherlands. E-mail: ctkbvi@xs4all.nl